

Joint inversion of airborne magnetic and electromagnetic data: case study in the Northwest Territories of Canada

Yue Zhu*, University of Utah, Michael S. Zhdanov, University of Utah, TechnoImaging and MIPT

Summary

One of the major challenges in interpretation of airborne geophysical data is the ability to jointly invert multiple geophysical datasets to self-consistent 3D earth models of physical properties that can subsequently be used for mapping the mineral deposits. In practice, empirical or statistical correlations between different physical properties may exist, but their specific forms may be unknown. In addition, there could be both analytical and structural correlations between different attributes of the model parameters. There is a need to develop joint inversion methodologies which would not require a priori knowledge about specific empirical or statistical relationships between the different physical parameters and/or their attributes. To this end, Zhdanov et al. (2012a) have recently developed a generalized theoretical framework for joint inversion using Gramian constraints. In this paper, we apply this general method to the solution of the problem of joint inversion of TMI and EM data. The case study of the joint inversion of airborne magnetic and electromagnetic data in the area of the Northwest Territories of Canada has demonstrated that joint inversion with Gramian constraints recovered the higher remanent magnetization typical of kimberlite pipes.

Introduction

Different geophysical fields provide information about different physical properties of rock formations. In many cases this information is mutually complementary, which makes it natural to consider a joint inversion of different geophysical data. There is also a need for a method of joint inversion, which would not require a priori knowledge about specific empirical or statistical relationships between the different model parameters and/or their attributes.

In the paper by Zhdanov et al. (2012a) a new approach to the joint inversion of multimodal data using Gramian constraints was introduced. The Gramians are computed as determinants of the corresponding Gram matrices of the multimodal model parameters and/or their different attributes. The Gramian provides a measure of correlation between the different model parameters or their attributes. By imposing the additional requirement of the minimum of the Gramian in regularized inversion, we obtain multimodal inverse solutions with enhanced correlations between the different model parameters or their attributes.

It was demonstrated in the cited paper that this new approach includes, as special cases, the methods, based on correlation and/or structural constraints, within a more general unified technique of generalized joint inversion.

The approach based on Gramian constraints makes it possible, in addition to correlation and structural constraints, to consider in a unified way other types of properties of the model parameters, which may serve an important role in the fusion of multimodal inversions. We can use, for example, second derivatives of the model parameters, absolute values of the gradients and/or second derivatives of the model parameters, and any other transforms of the model parameters and their gradients. In the current paper, we extend this approach to joint inversion of total magnetic intensity (TMI) and electromagnetic (EM) airborne data.

Inversion of TMI data for the magnetization vector

Total magnetic intensity (TMI) data are standard deliverables in every airborne geophysical survey. Most 3D inversion methods are based on the assumption that there is no remanent magnetization, and they recovery a 3D magnetic susceptibility model (e.g., Li and Oldenburg, 1996, 2003; Portniaguine and Zhdanov, 2002). However, it is well established that in many geological areas the direction of magnetization in a rock differs from the direction of today's magnetic field, H_0 . This effect is manifested by a presence of the remanent magnetization in the rocks. In order to include both induced and remanent magnetization, we consider as the magnetic model parameter the magnetization vector, \mathbf{M} , rather than the scalar susceptibility. In this case, using discrete model parameters and discrete data, we can present the forward modeling operator for the anomalous TMI field, as the following matrix equation:

$$d^{(1)} = A^{(1)}m^{(1)}, \quad (1)$$

where $d^{(1)}$ is the N_d length vector of the observed TMI data, $m^{(1)}$ is the $3N_m$ length vector of magnetization vector components, and $A^{(1)}$ is a linear operator of the TMI forward modeling problem.

Inversion of equation (1) is ill posed, and its solution requires regularization (Tikhonov and Arsenin, 1977). We solve the linear inverse problem (1) using the Tikhonov parametric functional with a pseudo-quadratic stabilizer (Zhdanov, 2002):

$$P^\alpha(m^{(1)}, d^{(1)}) = \varphi(m^{(1)}) + \alpha S(m^{(1)}) \rightarrow \min, \quad (2)$$

where $\varphi(m^{(1)})$ is a misfit functional:

$$\varphi(m^{(1)}) = \|W_d A^{(1)}m^{(1)} - W_d d^{(1)}\|_D^2. \quad (3)$$

The term S is a stabilizing functional, based on minimum norm, minimum support, and/or minimum gradient support constraints, respectively (Zhdanov, 2002). We minimize equation (2) using the re-weighted regularized conjugate

Joint inversion of airborne magnetic and electromagnetic data

gradient (RRCG) method. The further details of this method can be found in Zhdanov (2002).

Inversion of the airborne EM data for conductivity distribution

Inversion of frequency domain airborne EM data is based on the same principles as the inversion of TMI data. The major difference is in forward modeling operator used for generating the synthetic airborne data required for the inversion. We solve the forward modeling problem for AEM data using a contraction integral equation (IE) method (Zhdanov, 2009).

One can represent the modeling of airborne EM data as follows:

$$d^{(2)} = A^{(2)}(m^{(2)}), \quad (4)$$

where $d^{(2)}$ is the N_d length vector of observed data, $m^{(2)}$ is the N_m length vector of the anomalous conductivities, $\Delta\sigma$; and $A^{(2)}$ is the nonlinear modeling EM operator.

The regularized solution of the nonlinear inverse problem (4) can be based on the same Tikhonov parametric functional (2), as we used above for the TMI inversion, with the only difference being that all upper indices (1) should be replaced for (2), as shown below:

$$P^\alpha(m^{(2)}, d^{(2)}) = \varphi(m^{(2)}) + \alpha S(m^{(2)}) \rightarrow \min, \quad (5)$$

A detailed description of the algorithm of the airborne EM data inversion can be found in Cox and Zhdanov (2008), Cox et al., (2010, 2012), and Zhdanov (2009).

Principles of joint inversion of TMI and EM data

In the joint inversion, we use two separate misfit functionals for the airborne TMI and EM data combined in the parametric functional by the Gramian constraint S_G . This parametric functional is defined as follows:

$$P^\alpha(m^{(1)}, m^{(2)}) = \varphi^{(1)}(m^{(1)}) + \varphi^{(2)}(m^{(2)}) + \alpha c_1 [S(m^{(1)}) + S(m^{(2)})] + \alpha c_2 S_G(Tm^{(1)}, Tm^{(2)}), \quad (6)$$

where the misfit functionals are given by the following formulas:

$$\varphi^{(i)}(m^{(i)}) = \|W_d^{(i)}(A^{(i)}(m^{(i)}) - d^{(i)})\|^2, \quad i = 1, 2, \quad (7)$$

The term $S_G(Tm^{(1)}, Tm^{(2)})$ is the Gramian constraint (Zhdanov et al., 2012a, b), which in a case of two physical properties can be written, using matrix notations, as follows:

$$S_G(Tm^{(1)}, Tm^{(2)}) = \begin{vmatrix} (Tm^{(1)}, Tm^{(1)}) & (Tm^{(1)}, Tm^{(2)}) \\ (Tm^{(2)}, Tm^{(1)}) & (Tm^{(2)}, Tm^{(2)}) \end{vmatrix}. \quad (8)$$

Coefficients c_1 and c_2 are the weighting coefficients determining the weights of the different stabilizers in the parametric functional. The operator, T , used in the Gramian constraint, S_G , represents some linear transformation of the

model parameters with (\cdot, \cdot) standing for the inner product in the corresponding Gramian space (Zhdanov et al., 2012a). In the case of T being the identity operator, expression (8) is simplified as follows:

$$S_G(m^{(1)}, m^{(2)}) = \begin{vmatrix} (m^{(1)}, m^{(1)}) & (m^{(1)}, m^{(2)}) \\ (m^{(2)}, m^{(1)}) & (m^{(2)}, m^{(2)}) \end{vmatrix} = \|m^{(1)}\|^2 \|m^{(2)}\|^2 [1 - \eta^2(m^{(1)}, m^{(2)})], \quad (9)$$

where the coefficient, η , can be treated as a correlation coefficient between two parameters, $m^{(1)}$ and $m^{(2)}$:

$$\eta(m^{(1)}, m^{(2)}) = \frac{(m^{(1)}, m^{(2)})}{\|m^{(1)}\| \|m^{(2)}\|}. \quad (10)$$

Expression (9) shows that the Gramian provides a measure of correlation between two parameters, $m^{(1)}$ and $m^{(2)}$. Indeed, the Gramian goes to zero, when the correlation coefficient is close to one, which corresponds to linear correlation. This property shows that by minimizing a parametric functional with the Gramian constraint, we enforce some linear correlation between the model parameters.

We use the re-weighted conjugate gradient method (Zhdanov, 2002) to minimize the parametric functional (6).

Numerical model study

We have conducted a numerical test of the developed method using a model of a rectangular conductive and magnetized block of the dimensions 100 m by 100 m by 50 m buried at a depth of 50 m (Figure 1). The block has a resistivity of 100 Ohm-m, while the homogeneous background half-space has a resistivity of 1000 Ohm-m. The magnetic properties of the block are characterized by the following intensity of magnetization

$$\mathbf{I} = H_0 \mathbf{M},$$

where magnetization vector, \mathbf{M} , has the following scalar components $(0.06\sqrt{2}, 0, 0.06\sqrt{2})$ in the conductive block.

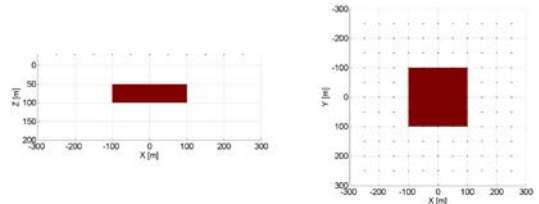


Figure 1: A sketch of the block model and receiver locations used in the synthetic model study. The receivers are located in the nodes over an 11 x 11 grid of 50-m spacing at 30 m above the ground.

We assume also that the magnitude of inducing magnetic field is equal to $H_0 = 50000$ nT, and the inclination and declination are as follows: $I = 75^\circ$ and $D = 15^\circ$. There are 121 receivers located in the nodes of 11 by 11 rectangular grid with 50 m spacing in both horizontal directions and 30 m above the ground, simulating an airborne survey. The

Joint inversion of airborne magnetic and electromagnetic data

receivers measure both the permanent magnetic anomalous field due to the block's magnetization and the frequency domain magnetic field due to EM Synthetic airborne magnetic TMI data were computer simulated, and 3% random noise was added to the TMI data as well.

The magnetic field data in the frequency domain were computer simulated using the IE method for the parameters of the DIGHEM airborne system, which measures five components of the magnetic field. The first three components were coplanar fields, representing the vertical magnetic field at three different frequencies, 56000, 7200 and 900 Hz, generated by a vertical magnetic dipole source. Another two components were the coaxial fields, representing the horizontal magnetic field along the flight direction at two frequencies, 5500 and 900 Hz, generated by a horizontal magnetic dipole source oriented along the flight line.

The joint inversion was applied with operator T being the identity operator, which implies that we directly correlate the magnetization vector with the anomalous conductivity. Figure 2 shows a comparison of the joint inversion results with those obtained from individual inversions. The individual magnetic inversion produces a diffused anomalous body with the magnitude of the magnetization vector significantly underestimated. By using the Gramian constraints in the joint inversion, we were able to reduce this ambiguity and produce the correct locations of the areas.

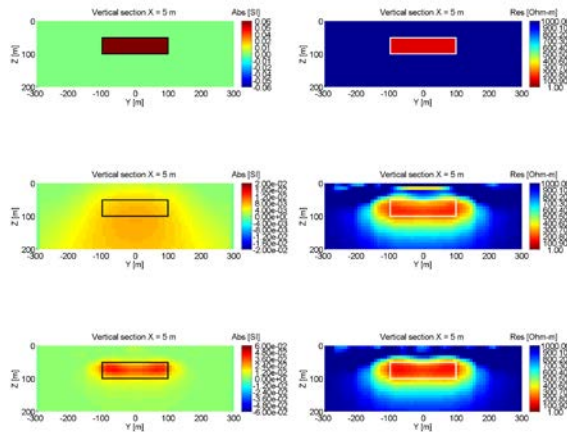


Figure 2: The recovered magnitude of the magnetization vector (left panels) and the resistivity (right panels) from the individual (middle panels) and joint (bottom panels) inversions with operator T being the identity matrix. The top panels show the vertical sections of the true model.

The anomalous magnetic body also became much more compact and reflected the shape of the anomalous domain

accurately. The recovered conductive anomaly also benefited from the joint inversion by improving the resolution of the conductive target. The artifacts in the very shallow area were greatly reduced as well.

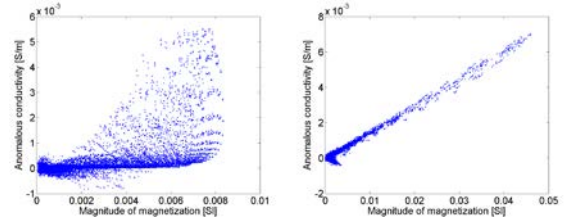


Figure 3: Cross plots of the magnitude of the magnetization vector versus anomalous conductivity from the separate inversions (left) and from the joint inversion (right) with the Gramian constraint with operator T being the identity operator.

Figure 3 presents the cross plots of the magnitude of the magnetization vector versus anomalous conductivity from the separate and joint inversions. One can see that the correlations between different physical parameters of the model has been improved dramatically by using the Gramian constraint.

Case study: joint inversion of airborne TMI and frequency domain EM data in the Northwest Territories of Canada

We have applied the developed joint inversion algorithm to the field airborne data collected for kimberlite exploration. The survey area belongs to the Slave Structural Province in the Northwest Territories of Canada, which forms a distinct cratonic block within the Canadian Precambrian Shield. The eastern domain of the Slave Geological Province, which underlies the Lac de Gras area, has been more productive for kimberlite exploration than the western domain. We have applied the joint inversion to total magnetic intensity (TMI) and frequency domain electromagnetic (EM) data collected over an area with the known kimberlite pipe.

In the first step of the analysis, independent inversions of the TMI and EM data sets were conducted.

Using the 1D AEM inversion result as the starting model and setting the half-space background conductivity as 10^{-5} S/m, we ran full 3D AEM inversion independently for subsurface resistivity distribution. We also ran a 3D inversion of the TMI data independently for the magnetization vector. Figure 4 shows the results of the independent 3D AEM inversion together with the recovered magnitude of magnetization vector produced by an independent TMI data inversion.

Joint inversion of airborne magnetic and electromagnetic data

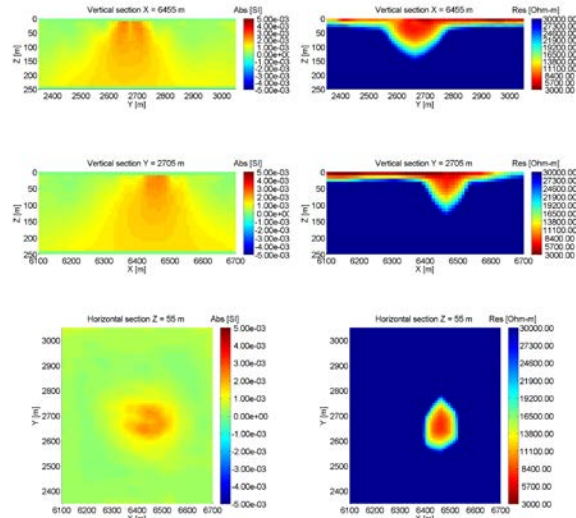


Figure 4: Vertical and horizontal sections of the inverse magnetization and resistivity models obtained by independent 3D inversions of the TMI and AEM data. The left panels present the magnitude of magnetization vector, while the right panels show the resistivity model in the survey area.

In the next step of our analysis, the joint inversion algorithm was applied to the airborne magnetic and electromagnetic data sets. The results of joint inversion with operator T being the identity matrix are shown in Figure 5. The cross plots, presented in Figure 6, show a strong correlation between the anomalous conductivity and the magnetization vector produced by a joint inversion with Gramian constraints.

Conclusions

In this paper, we have applied a general method of joint inversion using Gramian constraints to the solution of the problem of the joint inversion of TMI and EM data. This method does not require a priori knowledge about specific empirical or statistical relationships between the different physical parameters and/or their attributes, and instead determines these relationships, if they exist, in the process of the inversion. In addition, the Gramian approach could use both the statistical and structural correlations between different model parameters. We have demonstrated that the joint inversion for the conductivity and the magnetization vector works well even in the presence of the remanent magnetization. The case study of the joint inversion of airborne TMI and EM data in the area of the Northwest Territories of Canada has demonstrated that joint inversion with the Gramian constraints recovered the higher remanent magnetization typical of kimberlite pipes.

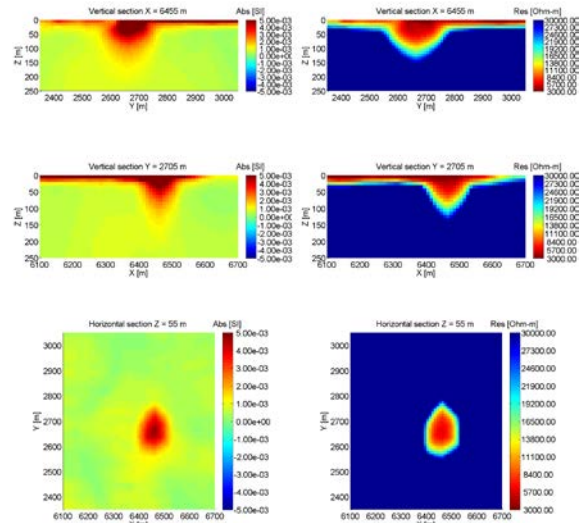


Figure 5: Vertical and horizontal sections of the inverse magnetization and resistivity models obtained by the joint 3D inversion of the TMI and AEM data with operator T being the identity matrix. The left panels present the magnitude of magnetization vector, while the right panels show the resistivity model in the survey area.

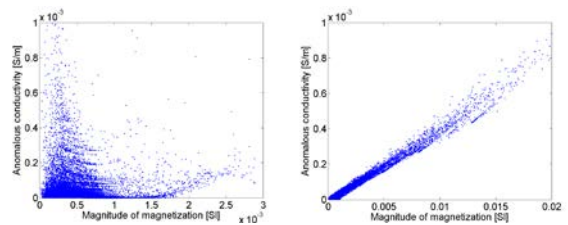


Figure 6: Cross plots of the magnitude of the magnetization vector versus anomalous conductivity from the separate inversions (left panel) and from the joint inversion (right panel) with the Gramian constraint with operator T being the identity operator.

Acknowledgement

The authors acknowledge CEMI and TechnoImaging for support of this research. We also acknowledge the Center for High Performance Computing, University of Utah, for providing computational resources. We also thank Leif Cox for his assistance with this project. We further acknowledge Rio Tinto for providing the data.

References

- Cox, L. H., and M. S. Zhdanov, 2008, Advanced computational methods for rapid and rigorous 3D inversion of airborne electromagnetic data: *Communications in Computational Physics*, **3**, 160-179.
- Cox, L. H., G. A. Wilson, and M. S. Zhdanov, 2010, 3D inversion of airborne electromagnetic data using a moving footprint: *Exploration Geophysics*, **41**, 250-259.
- Cox, L. H., G. A. Wilson, and M. S. Zhdanov, 2012, 3D inversion of airborne electromagnetic data: *Geophysics*, **77** (4), WB59-WB69.
- Li Y., and D. W. Oldenburg, 1996, 3-D inversion of magnetic data: *Geophysics*, **61**, 394-408. doi: 10.1190/1.1443968.
- Li Y., and D. W. Oldenburg, 2003, Fast inversion of large-scale magnetic data using wavelet transforms and a logarithmic barrier method: *Geophysical Journal International*, **152**, 251-265. doi: 10.1046/j.1365-246X.2003.01766.
- Portniaguine O., and M. S. Zhdanov, 2002, 3-D magnetic inversion with data compression and image focusing: *Geophysics*, **67**, 1532-1541. doi: 10.1190/1.1512749.
- Tikhonov, A. N., and V. Y. Arsenin, 1977, *Solution of ill-posed problems*: Winston and Sons.
- Zhdanov, M. S., 2002, *Geophysical inverse theory and regularization problems*: Elsevier.
- Zhdanov, M. S., 2009, *Geophysical electromagnetic theory and methods*: Elsevier.
- Zhdanov, M. S., A. V. Gribenko, and G. Wilson, 2012a, Generalized joint inversion of multimodal geophysical data using Gramian constraints: *Geophysical Research Letters*, **39**, L09301, 1-7.
- Zhdanov, M. S., A. V. Gribenko, G. Wilson, and C. Funk, 2012b, 3D joint inversion of geophysical data with Gramian constraints: A case study from the Carrapateena IOCG deposit, South Australia: *The Leading Edge*, **11**, 1382-1388.